Archive of Applied Mechanics 71 (2001) 207–220 © Springer-Verlag 2001

Control of transient thermoelastic displacement of a two-layered composite plate constructed of isotropic elastic and piezoelectric layers due to nonuniform heating

Y. Ootao, Y. Tanigawa

Summary In this study, the theoretical analysis of the control of transient thermoelastic displacement is developed for a two-layered composite rectangular plate constructed of an isotropic elastic and a piezoelectric layer due to nonuniform heat supply. The transient three-dimensional temperature in a two-layered composite rectangular plate is analyzed by the methods of Laplace and finite cosine transformations. Exact solutions for isotropic elastic and piezoelectric plates of crystal class mm2 are used in the theoretical analysis. A three-dimensional transient piezothermoelastic solution is developed for a simple-supported combined plate. The analysis yields an appropriate electric potential which when applied to the piezoelectric plate, suppresses the induced thermoelastic displacement in the thickness direction at the midpoint on the free surface of the isotropic plate. As an example, numerical calculations are carried out for an isotropic rectangular plate made of steel, bonded to a piezoelectric plate of cadmium selenide. Some numerical results are shown for temperature change, displacement and stress in transient state, when the transient thermoelastic displacement are controlled.

Key words piezothermoelasticity, displacement control, plate, transient state

1 Introduction

Piezoelectric materials exhibit coupled effects between the elastic and electric field, and have become of major interest lately as functional materials used in actuators or sensors [1]. It is possible to make a system of intelligent composite materials by combining piezoelectric materials with structural materials. Several analytical studies concerning piezothermoelasticity of intelligent composite materials have been reported. In particular, the control of thermoelastic displacements was treated in [2–7]. The piezothermoelastic problem concerning control of thermally induced elastic displacements of an isotropic plate with a piezoelectric plate of crystal class 6mm was investigated in [2–4]. In order to reduce the applied electric potential, the same piezothermoelastic problem concerning multiple piezoelectric plates of crystal class 6mm was investigated in [5]. The shape control of a cylindrical panel or a rectangular hybrid plate with some piezoelectric layers under thermomechanical load were reported in [6, 7], however, these papers are restricted to three-dimensional steady state piezothermoelastic problems.

It is well known that thermal stress distributions in transient states significantly differ from those in steady states. Therefore, we recently analyzed the three-dimensional transient piezothermoelastic problem for a rectangular composite plate composed of cross-ply and piezoelectric laminae, [8], and functionally graded rectangular plate bonded to a piezoelectric plate [9]. The numerical results for the temperature change, displacement, stress, electric potential and electric displacement distribution in a transient state under nonuniform heat supply were showed.

In the present paper, we analyze the transient three-dimensional piezothermoelastic problem of the control of thermoelastic displacements of a two-layered composite rectangular plate constructed of an isotropic elastic and a piezoelectric layer of crystal class mm2 due to

Received 27 December 1999; accepted for publication 1 August 2000

Y. Ootao (✉), Y. Tanigawa
Department of Mechanical Systems Engineering,
Osaka Prefecture University,
1-1 Gakuen-cho, Sakai 599-8531, Japan
E-mail: ootao@mecha.osakafu-u.ac.jp

nonuniform heat supply. The analysis of the problem leads to an appropriate electric potential applied to the piezoelectric plate which suppresses the induced thermoelastic displacement in the thickness direction at the midpoint on the free surface of the isotropic plate from the early stage of the heating to the steady state. Some numerical results for the temperature change, displacement and stress in a transient state are shown.

2 Theoretical development

2.1 Heat conduction problem

We consider a two-layered composite rectangular plate constructed of an isotropic elastic and a piezoelectric layer as shown in Fig. 1. The thicknesses of the elastic and the piezoelectric plates are represented by B and b, respectively. The lengths of the sides of the rectangular plate are denoted by $2L_x$ and $2L_y$, respectively. Coordinate axes x, y and z are chosen as shown in Fig. 1. Moreover, coordinate z_i represents a local coordinate system of ith layer, the origin of which is taken at the bottom side of the ith layer. Throughout the paper, the quantities with subscripts $i = 1$ and $i = 2$ denote those for the elastic and the piezoelectric plates, respectively. We assume that the two-layered composite plate is initially at zero temperature, and is suddenly heated nonuniformly from the bottom surface by surrounding medium, the temperature of which is denoted by the function $T_a f_a(x) g_a(y)$. The relative heat transfer coefficients on bottom and top surfaces of the combined plate are designated h_a and h_b, respectively. We assume that the end surfaces of the two-layered composite are held at zero temperature. Then, the transient heat conduction equation for the ith layer in dimensionless form is given as

$$\frac{\partial \bar{T}_1}{\partial \tau} = \bar{\kappa}\left(\frac{\partial^2 \bar{T}_1}{\partial \bar{x}^2} + \frac{\partial^2 \bar{T}_1}{\partial \bar{y}^2} + \frac{\partial^2 \bar{T}_1}{\partial \bar{z}_1^2}\right) , \tag{1}$$

$$\frac{\partial \bar{T}_2}{\partial \tau} = \bar{\kappa}_x \frac{\partial^2 \bar{T}_2}{\partial \bar{x}^2} + \bar{\kappa}_y \frac{\partial^2 \bar{T}_2}{\partial \bar{y}^2} + \bar{\kappa}_z \frac{\partial^2 \bar{T}_2}{\partial \bar{z}_2^2} , \tag{2}$$

and the initial and thermal boundary conditions in dimensionless form are taken in the following forms:

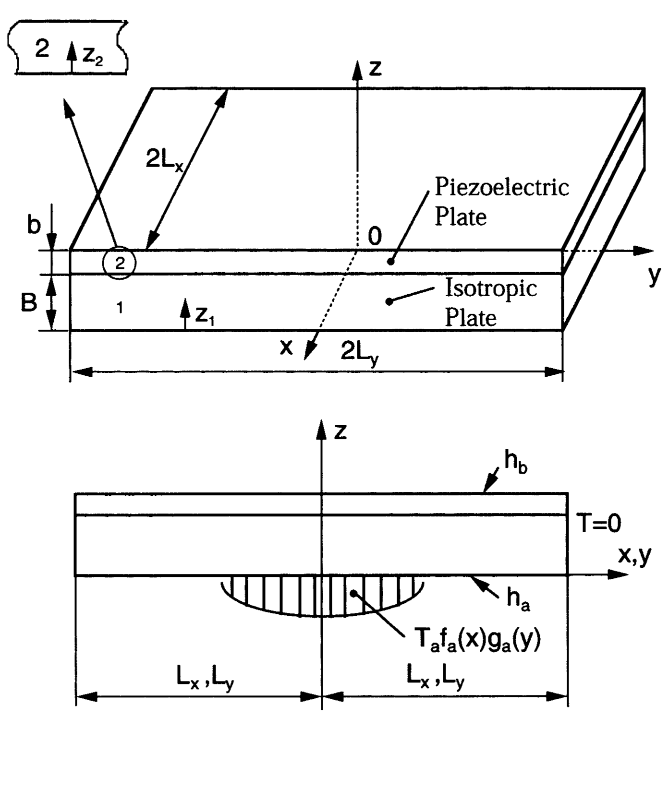

Fig. 1. Analytical model and coordinate system

$$\tau = 0, \quad \bar{T}_i = 0, \quad i = 1, 2 \ , \tag{3}$$

$$\bar{z}_1 = 0, \quad \frac{\partial \bar{T}_1}{\partial \bar{z}_1} - H_a \bar{T}_1 = -H_a \bar{T}_a f_a(\bar{x}) g_a(\bar{y}) \ , \tag{4}$$

$$\bar{z}_1 = 1, \quad \bar{z}_2 = 0, \quad \bar{T}_1 = \bar{T}_2 \ , \tag{5}$$

$$\bar{z}_1 = 1, \quad \bar{z}_2 = 0, \quad \bar{\lambda}_t \frac{\partial \bar{T}_1}{\partial \bar{z}_1} = \bar{\lambda}_{tz} \frac{\partial \bar{T}_2}{\partial \bar{z}_2} \ , \tag{6}$$

$$\bar{z}_2 = \bar{b}, \quad \frac{\partial \bar{T}_2}{\partial \bar{z}_2} + H_b \bar{T}_2 = 0 \ , \tag{7}$$

$$\bar{x} = \pm \bar{L}_x, \quad \bar{T}_i = 0, \quad i = 1, 2 \ , \tag{8}$$

$$\bar{y} = \pm \bar{L}_y, \quad \bar{T}_i = 0, \quad i = 1, 2 \ . \tag{9}$$

In expressions (1)–(9), we have introduced the following dimensionless values:

$$(\bar{T}_i, \bar{T}_a, \bar{T}_b) = \frac{(T_i, T_a, T_b)}{T_0}, \quad (\bar{L}_x, \bar{L}_y, \bar{b}) = \frac{(L_x, L_y, b)}{B}, \quad (\bar{x}, \bar{y}, \bar{z}, \bar{z}_i) = \frac{(x, y, z, z_i)}{B},$$
$$(\bar{\kappa}, \bar{\kappa}_k) = \frac{(\kappa, \kappa_k)}{\kappa_0}, \quad k = x, y, z, \quad (\bar{\lambda}_t, \bar{\lambda}_{tz}) = \frac{(\lambda_t, \lambda_{tz})}{\lambda_{t0}}, \quad \tau = \frac{\kappa_0 t}{B^2}, \quad (H_a, H_b) = (h_a, h_b) B \ , \tag{10}$$

where T_i is the temperature change of the ith layer, κ and κ_k $(k = x, y, z)$ are thermal diffusivity, λ_t and λ_{tz} are thermal conductivity, t is time and T_0, κ_0 and λ_{t0} are typical values of temperature, thermal diffusivity and thermal conductivity, respectively. The relation between the local coordinate $\bar{z}_i$ and the global coordinate $\bar{z}$ is given as follows:

$$\bar{z} = \bar{z}_i + (i - 1), \quad i = 1, 2 \ . \tag{11}$$

For the sake of brevity, we introduce the following symmetric conditions for the temperature functions $f_a(\bar{x})$ and $g_a(\bar{y})$ without loss of generality:

$$f_a(-\bar{x}) = f_a(\bar{x}), \quad g_a(-\bar{y}) = g_a(\bar{y}) \ . \tag{12}$$

Introducing the finite cosine transformations with respect to the variables $\bar{x}$ and $\bar{y}$ and the Laplace transformation with respect to the variable τ, the solution of Eqs. (1) and (2) can be obtained so as to satisfy conditions (3)–(10). This solution is shown as follows:

$$\bar{T}_i = \sum_{k=1}^{\infty} \sum_{l=1}^{\infty} \bar{T}_{ikl} \cos q_k \bar{x} \cos s_l \bar{y}, \quad i = 1, 2 \ , \tag{13}$$

where

$$\begin{aligned} \bar{T}_{ikl} = \frac{4}{\bar{L}_x \bar{L}_y} \Bigg[& \frac{1}{D} \left(\bar{A}_i' \cosh \rho_{kl} \bar{z}_i + \bar{B}_i' \sinh \rho_{kl} \bar{z}_i \right) \\ & + \sum_{j=1}^{m} \frac{2 \exp(-\omega_j^2 \tau)}{\omega_j \Delta'(\omega_j)} \left(\bar{A}_i \cosh \beta_{ij} \bar{z}_i + \bar{B}_i \sinh \beta_{ij} \bar{z}_i \right) \\ & + \sum_{j=m+1}^{\infty} \frac{2 \exp(-\omega_j^2 \tau)}{\omega_j \Delta'(\omega_j)} \left(\bar{A}_i \cos \gamma_{ij} \bar{z}_i + \bar{B}_i \sin \gamma_{ij} \bar{z}_i \right) \Bigg] \ , \end{aligned} \tag{14}$$

where Δ is a determinant of the 4×4 matrix $[a_{kl}]$, and the coefficients $\bar{A}_i$ and $\bar{B}_i$ are defined as the determinant of the matrix which is similar to the coefficient matrix $[a_{kl}]$ but in which the

$(2i-1)$th column or $2i$th column is exchanged by the constant vector $\{c_k\}$. The nonzero element a_{kl} and c_k among the coefficient matrix $[a_{kl}]$ and the constant vector $\{c_k\}$ are given from Eqs. (4–7). In Eqs. (13) and (14), quantities $q_k,\ s_l,\ \Delta'(\omega_j),\ \rho_{kl},\ \beta_{ij}$ and γ_{ij} are

$$
\begin{aligned}
& q_k = \frac{(2k-1)\pi}{2\bar{L}_x}, \quad s_l = \frac{(2l-1)\pi}{2\bar{L}_y}, \quad \Delta'(\omega_j) = \mathrm{d}\Delta/\mathrm{d}\omega|_{\omega=\omega_j}, \\
& \rho_{kl} = \sqrt{q_k^2 + s_l^2}, \quad i = 1, \\
& \rho_{kl} = \sqrt{(\bar{\kappa}_x q_k^2 + \bar{\kappa}_y s_l^2)/\bar{\kappa}_z}, \quad i = 2, \\
& \beta_{ij}^2 = -\left(\frac{\omega_j^2}{\bar{\kappa}} - q_k^2 - s_l^2\right) \quad \text{if } i = 1 \text{ and } \frac{\omega_j^2}{\bar{\kappa}} - q_k^2 - s_l^2 < 0, \\
& \gamma_{ij}^2 = \frac{\omega_j^2}{\bar{\kappa}} - q_k^2 - s_l^2 \quad \text{if } i = 1 \text{ and } \frac{\omega_j^2}{\bar{\kappa}} - q_k^2 - s_l^2 > 0, \\
& \beta_{ij}^2 = -\frac{\omega_j^2 - \bar{\kappa}_x q_k^2 - \bar{\kappa}_y s_l^2}{\bar{\kappa}_z} \quad \text{if } i = 2 \text{ and } (\omega_j^2 - \bar{\kappa}_x q_k^2 - \bar{\kappa}_y s_l^2) < 0, \\
& \gamma_{ij}^2 = \frac{\omega_j^2 - \bar{\kappa}_x q_k^2 - \bar{\kappa}_y s_l^2}{\bar{\kappa}_z} \quad \text{if } i = 2 \text{ and } (\omega_j^2 - \bar{\kappa}_x q_k^2 - \bar{\kappa}_y s_l^2) > 0 \ ,
\end{aligned}
\tag{15}
$$

and ω_j represent the jth positive roots of the following transcendental equation:

$$
\Delta(\omega) = 0 \ . \tag{16}
$$

The condition for the eigenvalue ω_j is given as

$$
\begin{aligned}
& \omega_1 < \omega_2 < \cdots < \omega_m < \sqrt{\bar{\kappa}\left(q_k^2 + s_l^2\right)} < \omega_{m+1} < \cdots \quad \text{if } i = 1, \\
& \omega_1 < \omega_2 < \cdots < \omega_m < \sqrt{\bar{\kappa}_x q_k^2 + \bar{\kappa}_y s_l^2} < \omega_{m+1} < \cdots \quad \text{if } i = 2 \ .
\end{aligned}
\tag{17}
$$

The details of the steady-temperature solution are omitted here for the sake of brevity.

2.2 Piezothermoelastic problem

We now develop the three-dimensional analysis for transient piezothermoelasticity in a simply supported two-layered composite rectangular plate constructed of an isotropic elastic and a piezoelectric layer.

In the piezoelectric plate, the stress–strain relations are expressed in dimensionless form as follows:

$$
\begin{Bmatrix} \bar{\sigma}_{xx2} \\ \bar{\sigma}_{yy2} \\ \bar{\sigma}_{zz2} \\ \bar{\sigma}_{yz2} \\ \bar{\sigma}_{zx2} \\ \bar{\sigma}_{xy2} \end{Bmatrix}
=
\begin{bmatrix}
\bar{C}_{11} & \bar{C}_{12} & \bar{C}_{13} & 0 & 0 & 0 \\
\bar{C}_{12} & \bar{C}_{22} & \bar{C}_{23} & 0 & 0 & 0 \\
\bar{C}_{13} & \bar{C}_{23} & \bar{C}_{33} & 0 & 0 & 0 \\
0 & 0 & 0 & \bar{C}_{44} & 0 & 0 \\
0 & 0 & 0 & 0 & \bar{C}_{55} & 0 \\
0 & 0 & 0 & 0 & 0 & \bar{C}_{66}
\end{bmatrix}
\begin{Bmatrix} \varepsilon_{xx2} - \bar{\alpha}_x \bar{T}_2 \\ \varepsilon_{yy2} - \bar{\alpha}_y \bar{T}_2 \\ \varepsilon_{zz2} - \bar{\alpha}_z \bar{T}_2 \\ \bar{\gamma}_{yz2} \\ \bar{\gamma}_{zx2} \\ \bar{\gamma}_{xy2} \end{Bmatrix}
-
\begin{bmatrix}
0 & 0 & \bar{e}_{31} \\
0 & 0 & \bar{e}_{32} \\
0 & 0 & \bar{e}_{33} \\
0 & \bar{e}_{24} & 0 \\
\bar{e}_{15} & 0 & 0 \\
0 & 0 & 0
\end{bmatrix}
\begin{Bmatrix} \bar{E}_x \\ \bar{E}_y \\ \bar{E}_z \end{Bmatrix} \ .
\tag{18}
$$

The constitutive equations for the electric field are

$$
\bar{D}_x = \bar{e}_{15}\bar{\gamma}_{zx} + \bar{\eta}_{11}\bar{E}_x, \quad \bar{D}_y = \bar{e}_{24}\bar{\gamma}_{yz} + \bar{\eta}_{22}\bar{E}_y, \quad \bar{D}_z = \bar{e}_{31}\bar{\varepsilon}_{xx} + \bar{e}_{32}\bar{\varepsilon}_{yy} + \bar{e}_{33}\bar{\varepsilon}_{zz} + \bar{\eta}_{33}\bar{E}_z + \bar{p}_z\bar{T} \ . \tag{19}
$$

The relations between the electric field intensities and the electric potential ϕ are defined by

$$\bar{E}_x = -\bar{\phi}_{,\bar{x}}, \quad \bar{E}_y = -\bar{\phi}_{,\bar{y}}, \quad \bar{E}_z = -\bar{\phi}_{,\bar{z}} \ , \tag{20}$$

where a comma denotes partial differentiation with respect to the variable which follows. If the free charge is absent, the equation of electrostatics is expressed in dimensionless form as follows:

$$\bar{D}_{x,\bar{x}} + \bar{D}_{y,\bar{y}} + \bar{D}_{z,\bar{z}} = 0 \ . \tag{21}$$

Substituting Eq. (20) and the displacement–strain relations into Eqs. (18) and (19), and later into the equilibrium equations and Eq. (21), the governing equations of the displacement components and the electric potential ϕ in dimensionless form are written as

$$\begin{aligned}
&\bar{C}_{11}\bar{u}_{2,\overline{xx}} + \bar{C}_{66}\bar{u}_{2,\overline{yy}} + \bar{C}_{55}\bar{u}_{2,\overline{zz}} + (\bar{C}_{12} + \bar{C}_{66})\bar{v}_{2,\overline{xy}} + (\bar{C}_{13} + \bar{C}_{55})\bar{w}_{2,\overline{xz}} + (\bar{e}_{31} + \bar{e}_{15})\bar{\phi}_{,\overline{xz}} \\
&\quad = \left(\bar{C}_{11}\bar{\alpha}_x + \bar{C}_{12}\bar{\alpha}_y + \bar{C}_{13}\bar{\alpha}_z\right)\bar{T}_{2,\bar{x}}, \\
&(\bar{C}_{66} + \bar{C}_{12})\bar{u}_{2,\overline{xy}} + \bar{C}_{66}\bar{v}_{2,\overline{xx}} + \bar{C}_{22}\bar{v}_{2,\overline{yy}} + \bar{C}_{44}\bar{v}_{2,\overline{zz}} + (\bar{C}_{23} + \bar{C}_{44})\bar{w}_{2,\overline{yz}} + (\bar{e}_{32} + \bar{e}_{24})\bar{\phi}_{,\overline{yz}} \\
&\quad = \left(\bar{C}_{12}\bar{\alpha}_x + \bar{C}_{22}\bar{\alpha}_y + \bar{C}_{23}\bar{\alpha}_z\right)\bar{T}_{2,\bar{y}}, \\
&(\bar{C}_{13} + \bar{C}_{55})\bar{u}_{2,\overline{xz}} + (\bar{C}_{44} + \bar{C}_{23})\bar{v}_{2,\overline{yz}} + \bar{C}_{55}\bar{w}_{2,\overline{xx}} + \bar{C}_{44}\bar{w}_{2,\overline{yy}} + \bar{C}_{33}\bar{w}_{2,\overline{zz}} + \bar{e}_{15}\phi_{,\overline{xx}} \\
&\quad + \bar{e}_{24}\phi_{,\overline{yy}} + \bar{e}_{33}\phi_{,\overline{zz}} = \left(\bar{C}_{13}\bar{\alpha}_x + \bar{C}_{23}\bar{\alpha}_y + \bar{C}_{33}\bar{\alpha}_z\right)\bar{T}_{2,\bar{z}}, \\
&(\bar{e}_{15} + \bar{e}_{31})\bar{u}_{2,\overline{xz}} + (\bar{e}_{24} + \bar{e}_{32})\bar{v}_{2,\overline{yz}} + \bar{e}_{15}\bar{w}_{2,\overline{xx}} + \bar{e}_{24}\bar{w}_{2,\overline{yy}} + \bar{e}_{33}\bar{w}_{2,\overline{zz}} - \bar{\eta}_{11}\bar{\phi}_{,\overline{xx}} \\
&\quad - \bar{\eta}_{22}\bar{\phi}_{,\overline{yy}} - \bar{\eta}_{33}\bar{\phi}_{,\overline{zz}} = -\bar{p}_z\bar{T}_{2,\bar{z}} \ .
\end{aligned} \tag{22}$$

In the case of the elastic plate, the displacement equations of equilibrium are written as

$$\begin{aligned}
&\left(\bar{\lambda} + 2\bar{\mu}\right)\bar{u}_{1,\overline{xx}} + \bar{\mu}\left(\bar{u}_{1,\overline{yy}} + \bar{u}_{1,\overline{zz}}\right) + \left(\bar{\lambda} + \bar{\mu}\right)\left(\bar{v}_{1,\overline{xy}} + \bar{w}_{1,\overline{xz}}\right) = \left(3\bar{\lambda} + 2\bar{\mu}\right)\bar{\alpha}\bar{T}_{1,\bar{x}}, \\
&\left(\bar{\lambda} + \bar{\mu}\right)\left(\bar{u}_{1,\overline{xy}} + \bar{w}_{1,\overline{yz}}\right) + \bar{\mu}\left(\bar{v}_{1,\overline{xx}} + \bar{v}_{1,\overline{zz}}\right) + \left(\bar{\lambda} + 2\bar{\mu}\right)\bar{v}_{1,\overline{yy}} = \left(3\bar{\lambda} + 2\bar{\mu}\right)\bar{\alpha}\bar{T}_{1,\bar{y}}, \\
&\left(\bar{\lambda} + \bar{\mu}\right)\left(\bar{u}_{1,\overline{xz}} + \bar{v}_{1,\overline{yz}}\right) + \bar{\mu}\left(\bar{w}_{1,\overline{xx}} + \bar{w}_{1,\overline{yy}}\right) + \left(\bar{\lambda} + 2\bar{\mu}\right)\bar{w}_{1,\overline{zz}} = \left(3\bar{\lambda} + 2\bar{\mu}\right)\bar{\alpha}\bar{T}_{1,\bar{z}} \ .
\end{aligned} \tag{23}$$

If the bottom and top surfaces of the combined plate are traction free, and the interface of the two layers are perfectly bonded then the boundary conditions of bottom and top surfaces and the conditions of continuity at the interface can be represented as follows:

$$\begin{aligned}
&\bar{z}_1 = 0 : \bar{\sigma}_{zz1} = 0, \quad \bar{\sigma}_{zx1} = 0, \quad \bar{\sigma}_{yz1} = 0, \\
&\bar{z}_1 = 1 : \bar{z}_2 = 0 : \bar{\sigma}_{zz1} = \bar{\sigma}_{zz2}, \quad \bar{\sigma}_{zx1} = \bar{\sigma}_{zx2}, \quad \bar{\sigma}_{yz1} = \bar{\sigma}_{yz2}, \\
&\qquad \bar{u}_1 = \bar{u}_2, \quad \bar{v}_1 = \bar{v}_2, \quad \bar{w}_1 = \bar{w}_2, \\
&\bar{z}_2 = \bar{b} : \bar{\sigma}_{zz2} = 0, \quad \bar{\sigma}_{zx2} = 0, \quad \bar{\sigma}_{yz2} = 0 \ .
\end{aligned} \tag{24}$$

The boundary conditions in the thickness direction for the electric field are expressed by

$$\bar{z}_2 = 0 : \bar{\phi} = 0 \ , \tag{25}$$

$$\bar{z}_2 = \bar{b} : \bar{\phi} = \bar{V}_0(\tau)F(\bar{x})G(\bar{y}) \ . \tag{26}$$

We now consider the case of a simply supported plate and assume that the end surfaces of the piezoelectric rectangular layer are electrically grounded. The boundary conditions are given as follows:

$$\begin{aligned}
&\bar{x} = \pm\bar{L}_x : \bar{\sigma}_{xxi} = 0, \ \ \bar{v}_i = 0, \ \ \bar{w}_i = 0, \ \ \bar{\phi} = 0, \\
&\bar{y} = \pm\bar{L}_y : \bar{\sigma}_{yyi} = 0, \ \ \bar{u}_i = 0, \ \ \bar{w}_i = 0, \ \ \bar{\phi} = 0 \ .
\end{aligned} \tag{27}$$

In expressions (18–27), we have introduced the following dimensionless values:

$$\bar{\sigma}_{kli} = \frac{\sigma_{kli}}{\alpha_0 Y_0 T_0}, \quad (\bar{\varepsilon}_{kli}, \bar{\gamma}_{kli}) = \frac{(\varepsilon_{kli}, \gamma_{kli})}{\alpha_0 T_0}, \quad (\bar{u}_i, \bar{v}_i, \bar{w}_i) = \frac{(u_i, v_i, w_i)}{\alpha_0 T_0 B},$$
$$(\bar{\alpha}, \bar{\alpha}_k) = \frac{(\alpha, \alpha_k)}{\alpha_0}, \quad \bar{C}_{kl} = \frac{C_{kl}}{Y_0}, \quad \bar{E}_k = \frac{E_k |d_1|}{\alpha_0 T_0}, \quad \bar{D}_k = \frac{D_k}{\alpha_0 Y_0 T_0 |d_1|}, \quad (\bar{\phi}, \bar{V}_0) = \frac{(\phi, V_0)|d_1|}{\alpha_0 T_0 B},$$
$$\bar{e}_{kl} = \frac{e_{kl}}{Y_0 |d_1|}, \quad \bar{\eta}_{kl} = \frac{\eta_{kl}}{Y_0 |d_1|^2}, \quad \bar{p}_z = \frac{p_z}{\alpha_0 Y_0 |d_1|}, \quad \bar{\lambda} = \frac{\lambda}{Y_0}, \quad \bar{\mu} = \frac{\mu}{Y_0}, \tag{28}$$

where σ_{kli} is the stress component, ε_{kli} is the normal strain component, γ_{kli} is the shearing strain component, $(u_i, v_i, w_i)$are the displacement components, α and α_k are the coefficients of linear thermal expansion, C_{kl} is the elastic stiffness constant, E_k is the electric field intensity, D_k is the electric displacement, e_{kl} is the piezoelectric coefficient, η_{kl} is the dielectric constant, p_z is the pyroelectric constant, d_1 is the piezoelectric modulus and α_0 and Y_0 are the typical values of the coefficient of linear thermal expansion and Young's modulus of elasticity, respectively, while λ and μ are Lamé's constants.

The boundary conditions (27) are satisfied automatically if the displacement components and electric potential are given in the following forms:

$$\begin{aligned}
\bar{u}_i &= \sum_{k=1}^{\infty}\sum_{l=1}^{\infty}\left[U_{cikl}(\bar{z}_i) + U_{pikl}(\bar{z}_i)\right] \sin q_k \bar{x} \, \cos s_l \bar{y}, \\
\bar{v}_i &= \sum_{k=1}^{\infty}\sum_{l=1}^{\infty}\left[V_{cikl}(\bar{z}_i) + V_{pikl}(\bar{z}_i)\right] \cos q_k \bar{x} \, \sin s_l \bar{y}, \\
\bar{w}_i &= \sum_{k=1}^{\infty}\sum_{l=1}^{\infty}\left[W_{cikl}(\bar{z}_i) + W_{pikl}(\bar{z}_i)\right] \cos q_k \bar{x} \, \cos s_l \bar{y}, \quad i = 1, 2, \\
\bar{\phi} &= \sum_{k=1}^{\infty}\sum_{l=1}^{\infty}\left[\Phi_{ckl}(\bar{z}_2) + \Phi_{pkl}(\bar{z}_2)\right] \cos q_k \bar{x} \, \cos s_l \bar{y} \ .
\end{aligned} \tag{29}$$

In expressions (29), the first term of the right-hand side shows the homogeneous solution of Eq. (22) or (23), and the second term of the right-hand side shows the particular solution of Eq. (22) or (23).

In the case of the elastic layer, $U_{cikl}(\bar{z}_i)$, $V_{cikl}(\bar{z}_i)$, and $W_{cikl}(\bar{z}_i)$ are given by the following expressions, [10]:

$$\begin{aligned}
U_{c1kl}(\bar{z}_1) &= \left(a_{11}^{(1)} + a_{31}^{(1)}\bar{z}_1 + a_{51}^{(1)}\bar{z}_1^2\right)\exp(\rho_{kl}\bar{z}_1) + \left(a_{21}^{(1)} + a_{41}^{(1)}\bar{z}_1 + a_{61}^{(1)}\bar{z}_1^2\right)\exp(-\rho_{kl}\bar{z}_1), \\
V_{c1kl}(\bar{z}_1) &= \left(a_{12}^{(1)} + a_{32}^{(1)}\bar{z}_1 + a_{52}^{(1)}\bar{z}_1^2\right)\exp(\rho_{kl}\bar{z}_1) + \left(a_{22}^{(1)} + a_{42}^{(1)}\bar{z}_1 + a_{62}^{(1)}\bar{z}_1^2\right)\exp(-\rho_{kl}\bar{z}_1), \\
W_{c1kl}(\bar{z}_1) &= \left(a_{13}^{(1)} + a_{33}^{(1)}\bar{z}_1 + a_{53}^{(1)}\bar{z}_1^2\right)\exp(\rho_{kl}\bar{z}_1) + \left(a_{23}^{(1)} + a_{43}^{(1)}\bar{z}_1 + a_{63}^{(1)}\bar{z}_1^2\right)\exp(-\rho_{kl}\bar{z}_1) \ .
\end{aligned} \tag{30}$$

In these expressions, $a_{kl}^{(1)}$ are unknown constants and the following relations among these constants exist:

$$\begin{aligned}
&a_{5l}^{(1)} = a_{6l}^{(1)} = 0 \quad l = 1, 2, 3, \\
&a_{32}^{(1)} = \frac{s_l}{q_k} a_{31}^{(1)}, \quad a_{33}^{(1)} = -\frac{\rho_{kl}}{q_k} a_{31}^{(1)}, \quad a_{42}^{(1)} = \frac{s_l}{q_k} a_{41}^{(1)}, \quad a_{43}^{(1)} = \frac{\rho_{kl}}{q_k} a_{41}^{(1)}, \\
&a_{31}^{(1)} = \frac{q_k(\bar{\lambda} + \bar{\mu})}{\rho_{kl}(\bar{\lambda} + 3\bar{\mu})}\left(q_k a_{11}^{(1)} + s_l a_{12}^{(1)} + \rho_{kl} a_{13}^{(1)}\right), \\
&a_{41}^{(1)} = -\frac{q_k(\bar{\lambda} + \bar{\mu})}{\rho_{kl}(\bar{\lambda} + 3\bar{\mu})}\left(q_k a_{21}^{(1)} + s_l a_{22}^{(1)} - \rho_{kl} a_{23}^{(1)}\right) \ .
\end{aligned} \tag{31}$$

In the case of the piezoelectric layer, $U_{cikl}(\bar{z}_i), V_{cikl}(\bar{z}_i), W_{cikl}(\bar{z}_i)$ and $\bar{\Phi}_{ckl}(\bar{z}_i)$ are given based on Heyliger's solution, [11]. Assuming that

$$\{U_{c2kl}(\bar{z}_2), V_{c2kl}(\bar{z}_2), W_{c2kl}(\bar{z}_2), \Phi_{ckl}(\bar{z}_2)\} = \left(U^0_{ckl}, V^0_{ckl}, W^0_{ckl}, \Phi^0_{ckl}\right) \exp(p\bar{z}_2) \quad , \tag{32}$$

and substituting the homogeneous solution into the homogeneous form of Eq. (22) leads to equations for $(U^0_{ckl}, V^0_{ckl}, W^0_{ckl}, \Phi^0_{ckl})$. From the condition that nontrivial solutions of these equations exist, an eighth-order equation for p is obtained. This equation can be written as the fourth-order equation

$$r^4 + cr^3 + dr^2 + er + f = 0 \quad , \tag{33}$$

where

$$\begin{aligned}
r &= p^2, \\
c &= \frac{1}{A}\left\{\bar{\eta}_{33}\left[\bar{C}_{44}\left(A_{11}\bar{C}_{33} - A_{13}^2\right) + \bar{C}_{55}\left(A_{33}\bar{C}_{44} + A_{22}\bar{C}_{33} - A_{23}^2\right)\right] + \bar{e}_{33}^2(A_{11}\bar{C}_{44} + A_{22}\bar{C}_{55})\right. \\
&\quad \left. + 2\bar{e}_{33}[\bar{C}_{55}(A_{34}\bar{C}_{44} - A_{23}A_{24}) - A_{13}A_{14}\bar{C}_{44}] + C_{33}\left[\bar{C}_{55}\left(A_{24}^2 - A_{44}\bar{C}_{44}\right) + A_{14}^2\bar{C}_{44}\right]\right\}, \\
d &= \frac{1}{A}\left\{\bar{\eta}_{33}\left[A_{11}A_{23}^2 + A_{13}^2A_{22} - 2A_{12}A_{23}A_{13} - A_{33}(A_{11}\bar{C}_{44} + A_{22}\bar{C}_{55}) + \bar{C}_{33}\left(A_{12}^2 - A_{11}A_{22}\right)\right]\right. \\
&\quad + 2\bar{e}_{33}(A_{13}A_{22}A_{14} + A_{11}A_{23}A_{24} - A_{12}A_{23}A_{14} - A_{12}A_{24}A_{13} - A_{11}A_{34}\bar{C}_{44} - A_{22}A_{34}\bar{C}_{55}) \\
&\quad + \bar{e}_{33}^2\left(A_{12}^2 - A_{11}A_{22}\right) + \bar{C}_{55}\left(2A_{23}A_{24}A_{34} + A_{22}A_{44}\bar{C}_{33} + A_{33}A_{44}\bar{C}_{44} - A_{23}^2A_{44} - A_{24}^2A_{33}\right. \\
&\quad \left.\left. - A_{34}^2\bar{C}_{44}\right) + \bar{C}_{44}\left(A_{11}A_{44}\bar{C}_{33} - A_{13}^2A_{44} + 2A_{13}A_{14}A_{34} - A_{14}^2A_{33}\right) + (A_{13}A_{24} - A_{14}A_{23})^2\right\}, \\
e &= \frac{1}{A}\left\{\left(A_{11}A_{22} - A_{12}^2\right)(\bar{\eta}_{33}A_{33} + 2\bar{e}_{33}A_{34} - \bar{C}_{33}A_{44}) + \left(A_{34}^2 - A_{33}A_{44}\right)(\bar{C}_{55}A_{22} + \bar{C}_{44}A_{11})\right. \\
&\quad + 2[A_{12}A_{24}(A_{13}A_{34} - A_{14}A_{33}) + A_{12}A_{23}(A_{14}A_{34} - A_{13}A_{44}) \\
&\quad \left. - A_{34}(A_{11}A_{23}A_{24} + A_{13}A_{22}A_{14})] + A_{33}\left(A_{11}A_{24}^2 + A_{14}^2A_{22}\right) + A_{44}\left(A_{13}^2A_{22} + A_{11}A_{23}^2\right)\right\}, \\
f &= \frac{1}{A}\left(A_{34}A_{44} - A_{34}^2\right)\left(A_{11}A_{22} - A_{12}^2\right), \\
A &= -\bar{C}_{55}\bar{C}_{44}\left(\bar{C}_{33}\bar{\eta}_{33} + \bar{e}_{33}^2\right) \quad .
\end{aligned} \tag{34}$$

$$\begin{aligned}
&A_{11} = \bar{C}_{11}q_k^2 + \bar{C}_{66}s_l^2, \quad A_{12} = (\bar{C}_{12} + \bar{C}_{66})q_k s_l, \quad A_{13} = (\bar{C}_{13} + \bar{C}_{55})q_k, \quad A_{14} = (\bar{e}_{31} + \bar{e}_{15})q_k, \\
&A_{22} = \bar{C}_{66}q_k^2 + \bar{C}_{22}s_l^2, \quad A_{23} = (\bar{C}_{23} + \bar{C}_{44})s_l, \quad A_{24} = (\bar{e}_{32} + \bar{e}_{24})s_l, \quad A_{33} = \bar{C}_{55}q_k^2 + \bar{C}_{44}s_l^2, \\
&A_{34} = \bar{e}_{15}q_k^2 + \bar{e}_{24}s_l^2, \quad A_{44} = -(\bar{\eta}_{11}q_k^2 + \bar{\eta}_{22}s_l^2) \quad .
\end{aligned} \tag{35}$$

For Eq. (33) there might be four real roots, two real roots and one pair of conjugate complex roots, or two pairs of conjugate complex roots. Piezoelectric material, which is considered in the next numerical calculation, corresponds to the case of four real roots. For this case, $U_{c2kl}(\bar{z}_2), V_{c2kl}(\bar{z}_2), W_{c2kl}(\bar{z}_2)$ and $\Phi_{ckl}(\bar{z}_2)$ are given by the following expressions:

$$\begin{aligned}
U_{c2kl}(\bar{z}_2) &= \sum_{J=1}^{4} U_{klJ}(\bar{z}_2), \quad V_{c2kl}(\bar{z}_2) = \sum_{J=1}^{4} L_{klJ}U_{klJ}(\bar{z}_2), \\
W_{c2kl}(\bar{z}_2) &= \sum_{J=1}^{4} M_{klJ}W_{klJ}(\bar{z}_2), \quad \Phi_{ckl}(\bar{z}_2) = \sum_{J=1}^{4} N_{klJ}W_{klJ}(\bar{z}_2) \quad ,
\end{aligned} \tag{36}$$

where

$$U_{klJ}(\bar{z}_2) = F_{klJ}C_{klJ}(\bar{z}_2) + G_{klJ}S_{klJ}(\bar{z}_2), \quad W_{klJ}(\bar{z}_2) = G_{klJ}C_{klJ}(\bar{z}_2) + \alpha_{klJ}F_{klJ}S_{klJ}(\bar{z}_2) \quad , \tag{37}$$

$$L_{klJ} = \frac{1}{D_J}\left(f_{11}m_J^4 + \alpha_{klJ}f_{12}m_J^2 + f_{13}\right), \quad M_{klJ} = \frac{m_J}{D_J}\left(f_{21}m_J^4 + \alpha_{klJ}f_{22}m_J^2 + f_{23}\right),$$
$$N_{klJ} = \frac{m_J}{D_J}\left(f_{31}m_J^4 + \alpha_{klJ}f_{32}m_J^2 + f_{33}\right), \quad D_J = \alpha_{klJ}g_1m_J^6 + g_2m_J^4 + \alpha_{klJ}g_3m_J^2 + g_4 \ , \tag{38}$$

$$C_{klJ}(\bar{z}_2) = \cosh(m_J\bar{z}_2), \quad S_{klJ}(\bar{z}_2) = \sinh(m_J\bar{z}_2), \quad m_J = \sqrt{\gamma_J}, \quad \alpha_{klJ} = 1 \quad \text{if } r_J > 0,$$
$$C_{klJ}(\bar{z}_2) = \cos(m_J\bar{z}_2), \quad S_{klJ}(\bar{Z}_2) = \sin(m_J\bar{z}_2), \quad m_J = \sqrt{-\gamma_J}, \quad \alpha_{klJ} = -1 \quad \text{if } r_J < 0 \ . \tag{39}$$

Here, F_{klJ} and G_{klJ} are unknown constants. Expressions for the coefficients in Eq. (38) and for the complex roots are omitted here for the sake of brevity.

On the other hand, $U_{pikl}(\bar{z}_i), V_{pikl}(\bar{z}_i), W_{pikl}(\bar{z}_i)$ and $\Phi_{pkl}(\bar{z}_i)$ of the particular solutions are obtained as the function system like the temperature solutions. The details of the particular solutions are omitted here.

In the case of the elastic plate, the stress components can be evaluated by substituting Eq. (29) into the displacement–strain relations, and later into the stress–strain relations. In the case of the piezoelectric plate, the stress components and the electric displacements can be evaluated by substituting Eq. (29) into the Eqs. (20) and the displacement–strain relations, and later into Eqs. (18) and (19). The unknown constants in Eqs. (30) and (37) are determined so as to satisfy the boundary conditions (24)–(26).

2.3 Control of transient thermoelastic displacement

We consider the control of the thermoelastic displacement in the thickness direction at the midpoint on the free surface of the elastic layer by an electric potential applied to the piezoelectric layer. First, we assume the functions $F(\bar{x})$ and $G(\bar{y})$ of Eq. (26). Next we decide the volume $\bar{V}_0(\tau_N)$ of Eq. (26) by repeated calculation, in order to reduce the induced thermoelastic displacement $\bar{w}$ at the midpoint on the free surface of the plate to zero in any discrete time τ_N from the early stage of the heating to the steady state.

3 Numerical results

To illustrate the foregoing analysis, we consider the piezoelectric layer, composed of cadmium selenide and the elastic layer composed of steel. Numerical results are presented for the following values:

$$H_a = H_b = 5.0, \quad \bar{T}_a = 1.0, \quad \bar{L}_x = \bar{L}_y = 3.0, \quad \bar{b} = 0.1,$$
$$f_a(\bar{x}) = \left(1 - \bar{x}^2/\bar{x}_0^2\right)H(\bar{x}_0 - |\bar{x}|), \quad g_a(\bar{y}) = \left(1 - \bar{y}^2/\bar{y}_0^2\right)H(\bar{y}_0 - |\bar{y}|), \quad \bar{x}_0 = 1.0, \quad \bar{y}_0 = 1.0,$$
$$\left.\begin{array}{l} F(\bar{x}) = \cos(\pi\bar{x}/2\bar{L}_x) \\ G(\bar{y}) = \cos(\pi\bar{y}/2\bar{L}_y) \end{array}\right\} \quad \text{case 1},$$
$$\left.\begin{array}{l} F(\bar{x}) = \cos^2(\pi\bar{x}/2\bar{L}_x) \\ G(\bar{y}) = \cos^2(\pi\bar{y}/2\bar{L}_y) \end{array}\right\} \quad \text{case 2} \ , \tag{40}$$

where $H(X)$ is the Heaviside's function. Material constants for steel are taken as

$$\lambda_1 = 51.6 \text{ W/m K}, \quad \kappa = 13.88 \times 10^{-6}\,\text{m}^2/\text{s}, \quad \alpha = 11.8 \times 10^{-6}\,\text{1/K},$$
$$Y = 206.0 \text{ Gpa}, \quad v = 0.3 \ , \tag{41}$$

and for cadmium selenide, [2],

$$\alpha_x = \alpha_y = 4.396 \times 10^{-6}\,\text{1/K}, \quad \alpha_z = 2.458 \times 10^{-6}\,\text{1/K}, \quad C_{11} = C_{22} = 74.1\,\text{GPa},$$
$$C_{12} = 45.2\,\text{GPa}, \quad C_{13} = C_{23} = 39.3\,\text{GPa}, \quad C_{33} = 83.6\,\text{GPa}, \quad C_{44} = C_{55} = 13.17\,\text{GPa},$$
$$C_{66} = 14.45\,\text{GPa}, \quad e_{31} = e_{32} = -0.16\,\text{C/m}^2, \quad e_{33} = 0.347\,\text{C/m}^2,$$

$$e_{15} = e_{24} = -0.138\,\mathrm{C/m^2}, \quad \eta_{11} = \eta_{22} = 8.25 \times 10^{-11}\,\mathrm{C^2/N\,m^2},$$
$$\eta_{33} = 9.03 \times 10^{-11}\,\mathrm{C^2/N\,m^2}, \quad p_z = -2.94 \times 10^{-6}\,\mathrm{C/m^2\,K}, \quad d_1 = -3.92 \times 10^{-12}\,\mathrm{C/N},$$
$$\lambda_{tx} = \lambda_{ty} = 8.6\,\mathrm{W/m\,K}, \quad \lambda_{tz} = 1.5\lambda_{tx} \ . \tag{42}$$

Since the coefficients of thermal conductivity for cadmium selenide could not be found in the literature, the following values are assumed:

$$\kappa_x = \kappa_y = 3.28 \times 10^{-6}\,\mathrm{m^2/s}, \quad \kappa_z = 1.5\kappa_x \ . \tag{43}$$

The typical values of material properties such as κ_0, λ_{t0}, α_0 and Y_0, used to normalize the numerical data, are based on those of steel.

Figure 2 shows the variation of the temperature change on the x-axis ($\bar{y} = 0$, $\bar{z} = 0$). The temperature rise can clearly be seen in the heated region. Figure 3 shows the variation with time of the applied electric potential $\bar{V}_0$ in order to reduce the induced thermolastic displacement $\bar{w}$ at the midpoint on the free surface of the plate to zero. The applied electric potential $\bar{V}_0$ in case 1 is small compared with that of case 2.

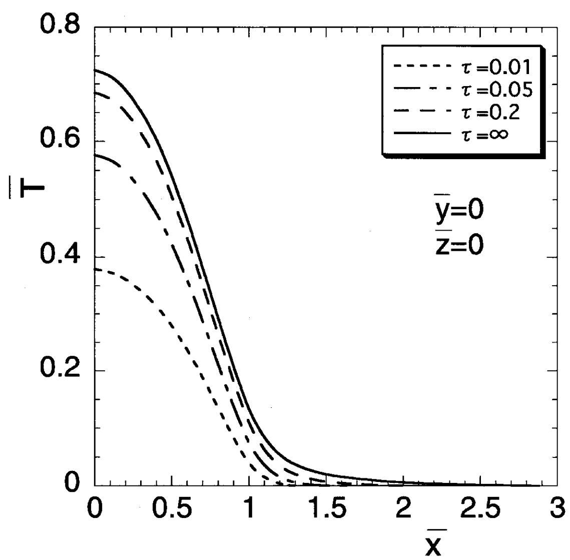

Fig. 2. Variation of temperature on the x-axis ($\bar{y} = 0$, $\bar{z} = 0$)

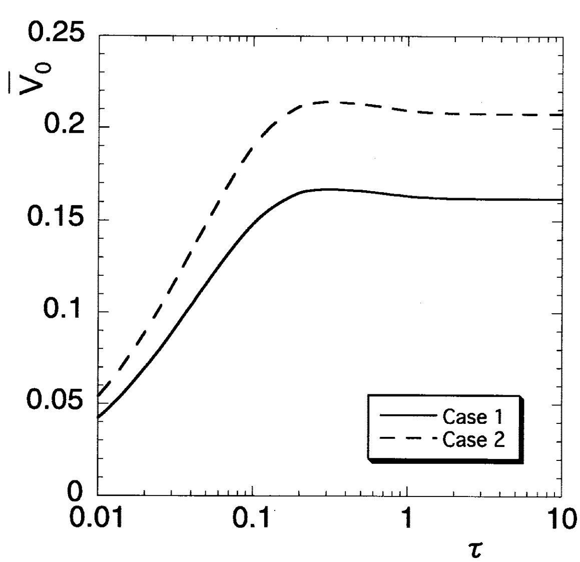

Fig. 3. Variation of the applied electric potential $\overline{V}_0$ with time (cases 1 and 2)

Figures 4–7 show the numerical calculations of case 1. Figure 4 shows the variation of the thermal displacement $\bar{w}$ on the x-axis ($\bar{y} = 0,\ \bar{z} = 0$), while Figs. 5 and 6 show the variations of the normal stresses $\bar{\sigma}_{xx}$ and $\bar{\sigma}_{zz}$ at the midpoint of the plate, respectively. As shown in Fig. 5, it can be seen that a discontinuity occurs on the interface between the elastic layer and the piezoelectric plate and large compressive stress occur in piezoelectric plate. As shown in Fig. 6, it can be seen that the stress variation becomes substantial with the progress of time and maximum tensile stress occurs in a transient state. Figure 7a and 7b show the distributions of normal stress $\bar{\sigma}_{zz}$ and shearing stress $\bar{\sigma}_{zx}$ on the interface ($\bar{y} = 0,\ \bar{z} = 1.0$), respectively.

Figures 8a and 8b show the numerical calculation for case 2. The distributions of normal stress $\bar{\sigma}_{zz}$ and shearing stress $\bar{\sigma}_{zx}$ on the interface ($\bar{y} = 0,\ \bar{z} = 1.0$) are shown in Figs. 8a and 8b, respectively. It can be seen from Figs. 7 and 8 that the distributions on the interface for case 2 are different from those of case 1.

In order to examine the influence of the shape control on the displacement and the stresses, the numerical results for the case when the deformation is not controlled are shown in Figs. 9, 10a and 10b. Figure 9 shows the variation of the thermal displacement $\bar{w}$ on the x-axis ($\bar{y} = 0,\ \bar{z} = 0$). Figures 10a and 10b show the variations of normal stress $\bar{\sigma}_{zz}$ and shearing stress $\bar{\sigma}_{zx}$ on the interface ($\bar{y} = 0,\ \bar{z} = 1.0$), respectively. When the deformation is not controlled, the numerical results are obtained by using the next boundary condition

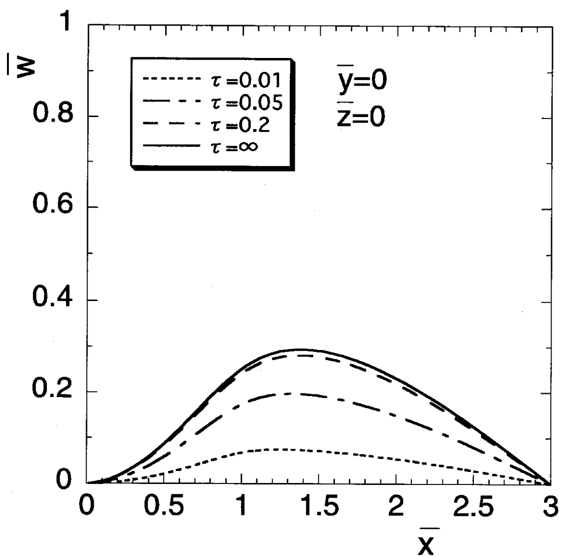

Fig. 4. Variation of thermal displacement $\bar{w}$ on the x-axis ($\bar{y} = 0,\ \bar{z} = 0$) (case 1)

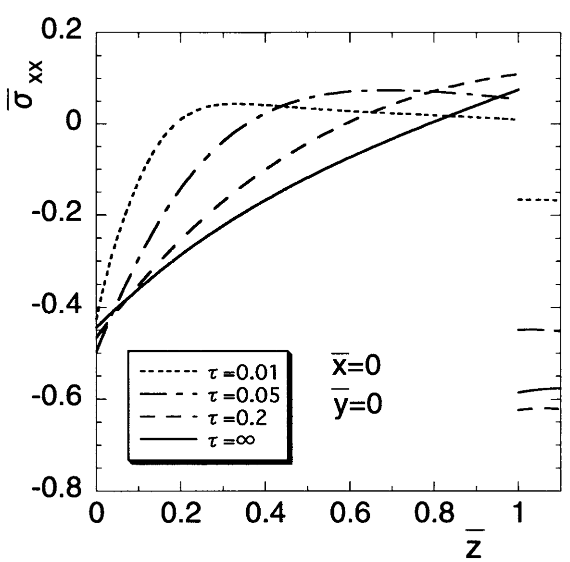

Fig. 5. Variation of thermal stress $\bar{\sigma}_{xx}$ ($\bar{x} = 0,\ \bar{y} = 0$) (case 1)

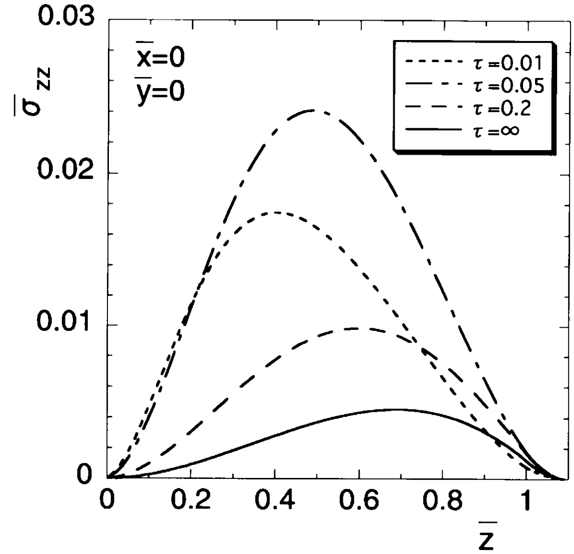

Fig. 6. Variation of thermal stress $\bar{\sigma}_{zz}$ ($\bar{x} = 0,\ \bar{y} = 0$) (case 1)

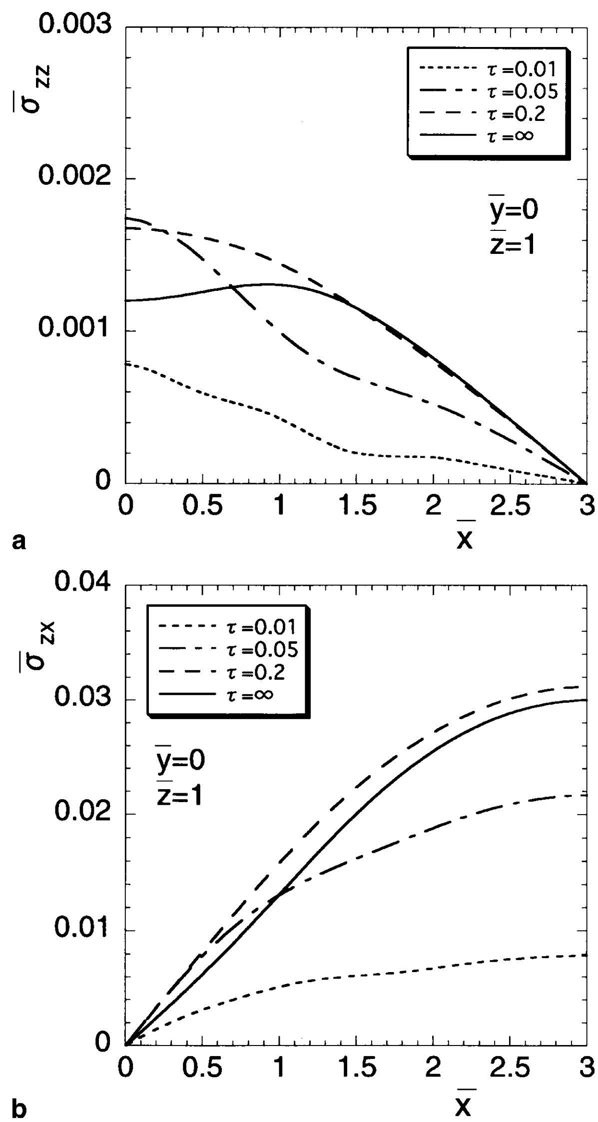

Fig. 7a, b. Variation of thermal stress on the interface ($\bar{y} = 0,\ \bar{z} = 1.0$) (case 1); **a** normal stress $\bar{\sigma}_{zz}$; **b** shearing stress $\bar{\sigma}_{zx}$

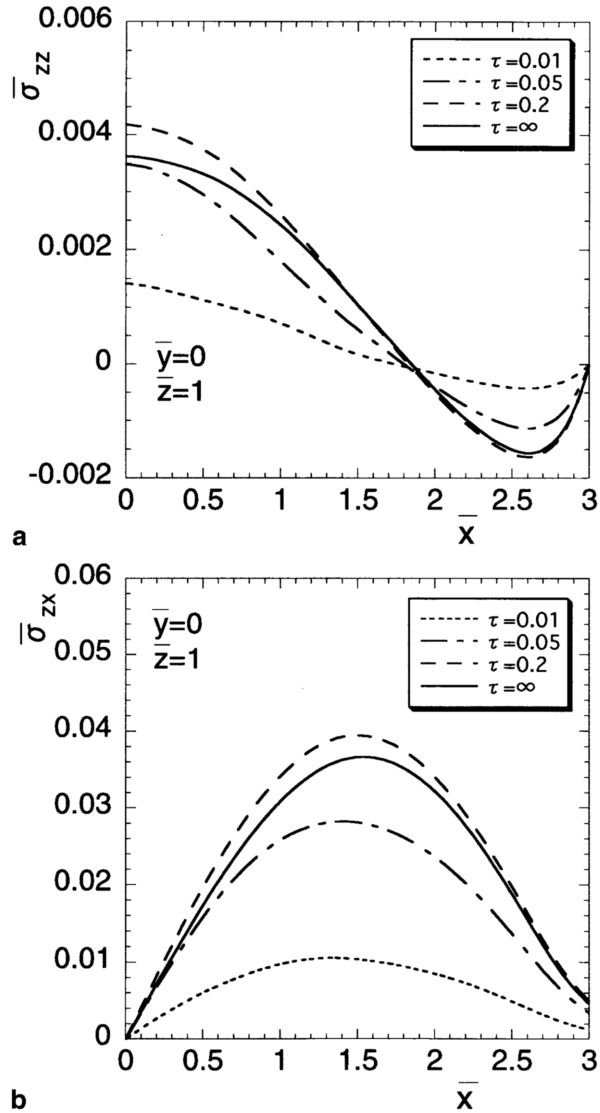

Fig. 8a, b. Variation of thermal stress on the interface ($\bar{y} = 0,\ \bar{z} = 1.0$) (case 2). **a** Normal stress $\bar{\sigma}_{zz}$; **b** shearing stress $\bar{\sigma}_{zx}$

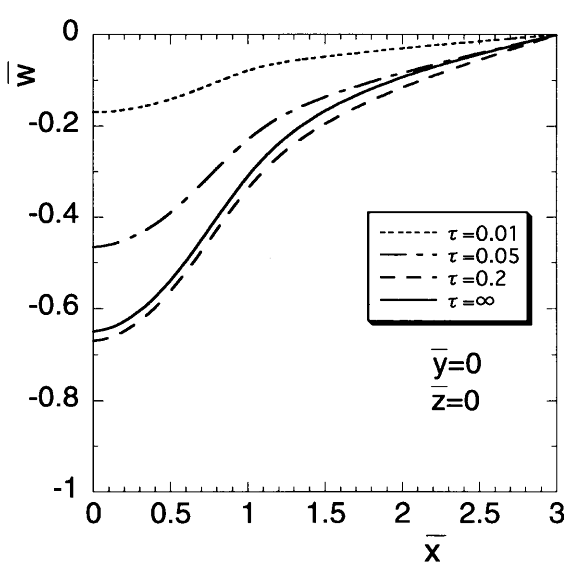

Fig. 9. Variation of thermal displacement $\overline{w}$ on the x-axis when the deformation is not controlled ($\bar{y} = 0,\ \bar{z} = 0$)

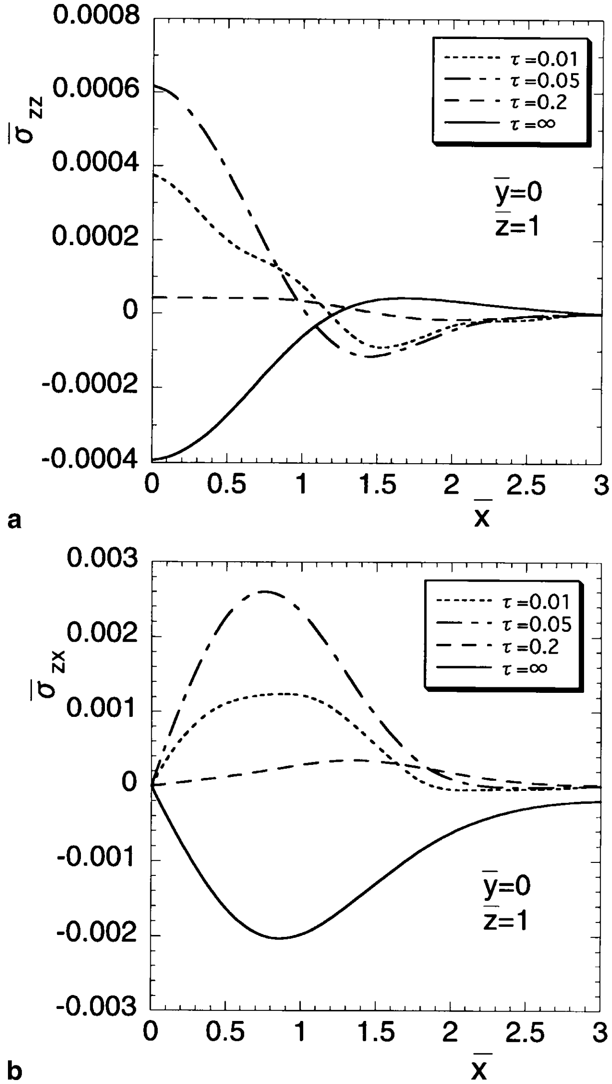

Fig. 10a, b. Variation of thermal stress on the interface when the deformation is not controlled ($\bar{y} = 0,\ \bar{z} = 1.0$). **a** Normal stress $\bar{\sigma}_{zz}$; **b** shearing stress $\bar{\sigma}_{zx}$

$$\bar{z}_2 = \bar{b}; \quad \bar{D}_z = 0 \ , \tag{44}$$

in place of Eq. (26). From Figs. 7, 8, and 10, it can be seen that when the deformation is controlled the stress distribution shows considerably larger values than that when the deformation is not controlled.

4 Concluding remarks

In this study, the theoretical analysis of the control of transient thermoelastic displacements is developed for a two-layered composite rectangular plate constructed of an elastic and a piezoelectric layer due to nonuniform heat supply. As an illustration, we carried out numerical calculations for the elastic layer of steel bonded to a piezoelectric plate of cadmium selenide, and examined the temperature change, the displacement and the stress distributions when the deformation is controlled. It is found that the transverse stress distribution on the interface when the deformation is controlled shows considerably larger values as compared with that when the deformation is not controlled.

References

1. **Sunar, M.; Rao, S.S.:** Recent advances in sensing and control of flexible structures via piezoelectric materials technology. Appl Mech Rev 52 (1999) 1–16
2. **Choi, J.-S.; Ashida, F.; Noda, N.:** Control of thermally induced elastic displacement of an isotropic structural plate bonded to a piezoelectric ceramic plate. Acta Mech 122 (1997) 49–63
3. **Ashida, F.; Noda, N.:** Control of transient thermoelastic displacement of an isotropic plate associated with a piezoelectric ceramic plate. J Thermal Stresses 20 (1997) 407–427

4. **Ashida, F.; Choi, J.-S.; Noda, N.:** Control of elastic displacement in piezoelectric-based intelligent plate subjected to thermal load. Int J Eng Sci 35 (1997) 851–868
5. **Ashida, F.:** Reduction of applied electric potential controlling thermoelastic displacement in a piezoelectric actuator. Arch Appl Mech 69 (1999) 443–454
6. **Kapuria, S.; Sengupta, S.; Dumir, P.C.:** Three-dimensional piezothermoelastic solution for shape control of cylindrical panel. J Thermal Stresses 20 (1997) 67–85
7. **Kapuria, S.; Dumir, P.C.; Sengupta, S.:** Three-dimensional solution for shape control of a simply supported rectangular hybrid plate. J Thermal Stresses 22 (1999) 159–176
8. **Ootao, Y.; Tanigawa, Y.:** Three-dimensional transient peizothermoelasticity for a rectangular composite plate composed of cross-ply and piezoelectric laminae. Int J Eng Sci 30 (2000) 47–71
9. **Ootao, Y.; Tanigawa, Y.:** Three-dimensional transient peizothermoelasticity in functionally graded rectangular plate bonded to a piezoelectric plate. Int J Solids Struct 37 (2000) 4377–4401
10. **Ootao, Y.; Tanigawa, Y.:** Three-dimensional transient thermal stresses of functionally graded rectangular plate due to partial heating. J Thermal Stresses 22 (1999) 35–55
11. **Heyliger, P.:** Exact solutions for simply supported laminated piezoelectric plates. ASME J Appl Mech 64 (1997) 299–306